Supplementary information

Influence of Cu induced crystallographic disorder on the optical and lattice vibrational properties of ZnO nanoparticles

Md. Abdullah Zubair[1]*, Tasnim Kamal Mouri[2], Mohammed Tareque Chowdhury[3]

[1]*Department of Nanomaterials and Ceramic Engineering, Bangladesh University of Engineering and Technology (BUET), Dhaka – 1000, Bangladesh*

[2]*Institute of Energy Conversion and Department of Materials Science and Engineering, University of Delaware, Newark, DE 19716, USA*

[3]*Institute of Energy Science, Atomic Energy Research Establishment, Bangladesh Atomic Energy Commission (BAEC), Dhaka – 1000, Bangladesh*

*Corresponding Author Email: mazubair2017@gmail.com (M. A. Zubair)

Supplementary note 1:

Table S1. Observed vibrational frequencies of different modes in 400°C annealed nanoparticles [1-5]

Vibrational frequency (cm^{-1})	Vibrational mode
~3400 – 3500	O – H stretching
~2925	$–CH_2–$ stretching
~2850	$–CH_3–$ stretching
~2340	CO_2 molecule
~1650 – 1550	H–O–H bending
	C – O symmetric & asymmetric bending
	Amino ($–NH_2$) group
~1390	COO^- symmetric stretching from metal (Zn) complex
1465, 1422 – 1350	$–CH_2–$ bending
1470 – 1430	$–CH_3–$ asymmetric
~1000 – 1100	Zn – OH stretching and deformation
	– CO stretching
	Other organic groups with Zn-hydroxy-acetate
~680	Cu – Zn – O stretching
~400 – 500	Zn – O stretching

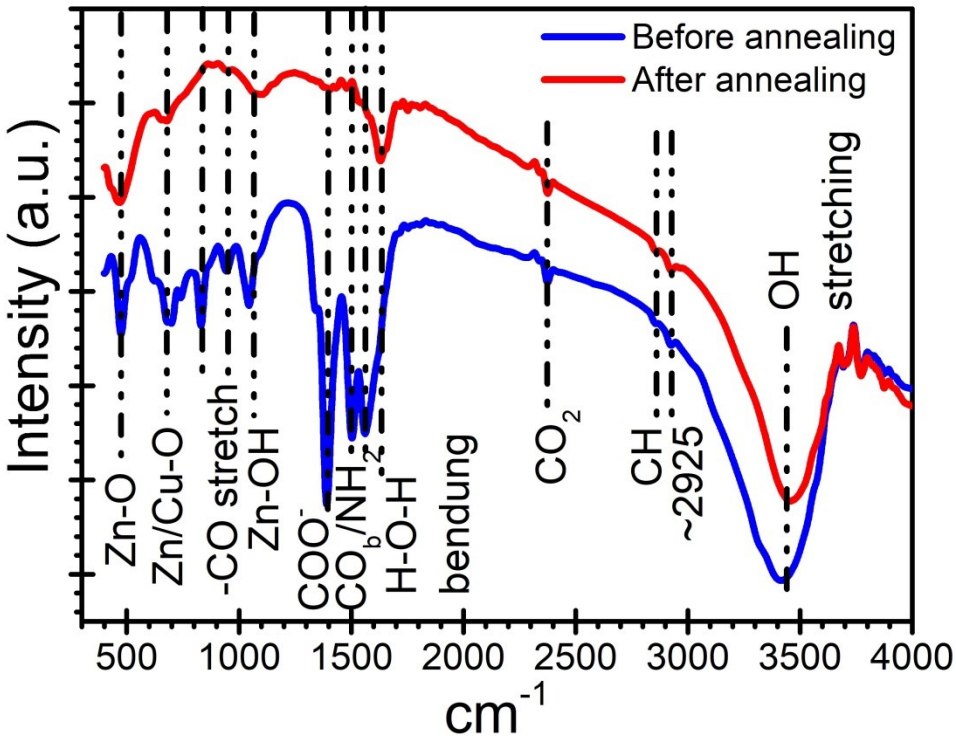

Fig. S1. A comparison between the typical FTIR spectra of 5% Cu incorporated ZnO before and after annealing, exhibiting strong suppression of associate with various complex forming organic group and hydroxyl group after annealing the dry precursor at 400^{o}C, leading to formation and enrichment of oxide phase. Similar type of noticeable suppression in absorption spectra has been observed for other samples. (Here, CO_b corresponds to symmetric and asymmetric vibration of CO)

Supplementary note 2:

Table. S2. EDX standard-less semi-quantitative elemental composition data

	EDX elemental composition in mass% with standard deviation			
	Cu	Zn	O	C
ZnO	-	73.5 ± 2.9	14.8 ± 1.9	10.3 ± 3.7
3% Cu_ZnO	1.8 ± 0.6	70.9 ± 2.6	17.7 ± 1.4	9.2 ± 2.5
5% Cu_ZnO	2.9 ± 0.8	71.3 ± 2.3	19.9 ± 1.8	5.9 ± 2.9
10% Cu_ZnO	6.5 ± 0.5	70.1 ± 2.9	21.2 ± 1.7	4.8 ± 2.7

Supplementary note 3:

Table. S3. Occupancy, atomic fractional coordinates and B_{iso} from Rietveld data

Atom	wyck	S.O.F*	x	y	z	B/10^4 pm^2
			ZnO			
O	2b	0.980000	0.333333	0.666667	0.3812(3)	0.7(1)
Zn	2b	1.000000	0.333333	0.666667	0.000000	0.29(2)
			3%Cu_ZnO			
O	2b	0.980000	0.333333	0.666667	0(1)	0.8(3)
Zn	2b	0.970000	0.333333	0.666667	0.000000	0.6(2)
Cu	2b	0.030000	0.333333	0.666667	0.000000	0.6(3)
			5%Cu_ZnO			
O	2b	0.995000	0.333333	0.666667	0(2)	0.6(5)
Zn	2b	0.950000	0.333333	0.666667	0.000000	0.7(4)
Cu	2b	0.050000	0.333333	0.666667	0.000000	0.5(4)
			10%Cu_ZnO			
O	2b	1.000000	0.333333	0.666667	0.4(2)	0.7(2)
Zn	2b	0.900000	0.333333	0.666667	0.000000	0.3(3)
Cu	2b	0.100000	0.333333	0.666667	0.000000	0.3(2)

*S.O.F: Site occupancy factor (fixed for Zn/Cu site in this report)

Supplementary note 4:

Table S4. Crystallographic parameters extracted from different models for X-ray line broadening analysis

Sample ID	ZnO	3%Cu ZnO	5%Cu ZnO	10%Cu ZnO
		Williamson Hall , UDM		
D (nm)	55.46	20.39	22.00	20.09
$\langle\varepsilon\rangle$	1.40×10^{-3}	1.50×10^{-3}	2.20×10^{-3}	2.40×10^{-3}
$*\vartheta$ (cm^{-2})	3.25×10^{10}	2.40×10^{11}	2.06×10^{11}	2.47×10^{11}
R^2	0.9996	0.9995	0.9996	0.9949
		Williamson Hall, USDM		
D (nm)	51.35	19.65	21.01	18.99
σ (MPa)	162	178	253.3	271.67
$**\langle\varepsilon\rangle_{avg.}$	$1.30(7)\times10^{-3}$	$1.42(8)\times10^{-3}$	$2.03(12)\times10^{-3}$	$2.17(12)\times10^{-3}$
ϑ (cm^{-2})	3.79×10^{10}	2.58×10^{11}	2.26×10^{11}	2.77×10^{11}
R^2	0.9771	0.9771	0.9971	0.9749
		Williamson Hall, UDEDM		
D (nm)	53.32	19.97	21.66	19.52
$‡^{\sigma_{avg.}}$ (MPa)	170(5)	187(6)	266 (8)	285(9)
$\langle\varepsilon\rangle_{avg.}$	$1.35(4)\times10^{-3}$	$1.49(4)\times10^{-3}$	$2.12(6)\times10^{-3}$	$2.27(7)\times10^{-3}$
u (J/m^3)	1.15×10^{5}	1.39×10^{5}	2.81×10^{5}	3.23×10^{5}
ϑ (cm^{-2})	3.51×10^{10}	2.50×10^{11}	2.13×10^{11}	2.62×10^{11}
R^2	0.9937	0.9937	0.9921	0.9903
		Size-Strain Plot (SSP)		
D (nm)	42.01	17.71	18.24	16.50
$\langle\varepsilon\rangle$	6.32×10^{-3}	9.15×10^{-3}	1.09×10^{-2}	1.26×10^{-2}
ϑ (cm^{-2})	3.52×10^{10}	3.18×10^{11}	3.00×10^{11}	3.67×10^{11}
R^2	0.9995	0.9999	0.9993	0.9990
		Approximation model		
D (nm)	49.58	19.00	22.06	20.65
$\langle\varepsilon\rangle$	1.56×10^{-3}	1.88×10^{-3}	2.87×10^{-3}	3.26×10^{-3}
ϑ (cm^{-2})	4.06×10^{10}	2.76×10^{11}	2.05×10^{11}	2.34×10^{11}

$*\,\vartheta = 1/D^2$ is the dislocation line density, $**\langle\varepsilon\rangle_{avg.}$ is the crystallographic average of micro-strain, $‡^{\sigma_{avg.}}$ is the crystallographic average of stress.

Supplementary note 5:

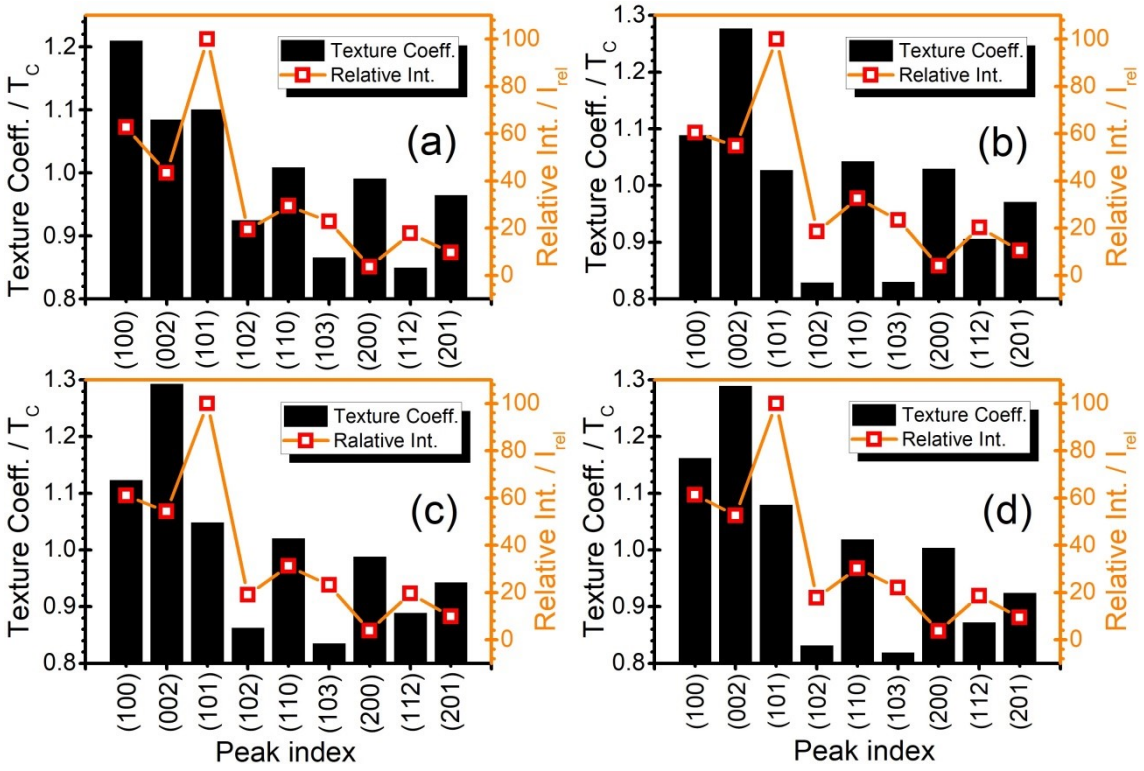

Fig. S2. Variation in Texture coefficient and relative peak intensity of the (hkl) diffraction planes for (a) ZnO (B) 3%Cu_ZnO (c) 5%Cu_ZnO and (d) 10%Cu_ZnO nanoparticles

The texture coefficient (T_C) of the individual crystallographic planes given in Table S2 above has been calculated using the equation given by [6]:

$$T_C = \frac{I_i(hkl)}{I_{oi}(hkl)} \times \left[\left(N^{-1}\right) \times \sum_{i=1}^{N} \frac{I_i(hkl)}{I_{oi}(hkl)} \right]^{-1} \qquad (1)$$

Where, $I_i(hkl)$ the measured intensity of the ith hkl plane, $I_{oi}(hkl)$ is the standard intensity of the ith hkl plane and N is the number of reflections. Here the values of $I_{oi}(hkl)$ were obtained from ICDD 01-080-3003 reference pattern.

Supplementary note 6:

Table. S5. Data for crystallite size and micro-strain calculation adopting the approximation method

Sample ID	ZnO	3%Cu_ZnO	5%Cu_ZnO	10%Cu_ZnO
2^{θ}_{100}(°)	31.755	31.801	31.772	31.765
2^{θ}_{101}(°)	36.242	36.279	36.246	36.240
β_{100}(rad)	4.213×10^{-3}	8.869×10^{-3}	9.001×10^{-3}	9.812×10^{-3}
β_{101}(rad)	4.494×10^{-3}	9.231×10^{-3}	9.522×10^{-3}	10.402×10^{-3}
β_{101}/β_{100}	1.066	1.041	1.058	1.060
m_{100}/β_{100}	0.690	0.855	0.747	0.732
n_{101}/β_{101}	0.456	0.268	0.395	0.410
m_{100}(rad)	2.907×10^{-3}	7.585×10^{-3}	6.723×10^{-3}	7.183×10^{-3}
n_{101}(rad)	2.049×10^{-3}	2.474×10^{-3}	3.761×10^{-3}	4.265×10^{-3}
D(nm)	49.585	19.006	21.441	20.070
$\langle\varepsilon\rangle$	1.565×10^{-3}	1.887×10^{-3}	2.873×10^{-3}	3.258×10^{-3}

Supplementary note 7:

Table. S6. Peak shape factors as a function of (hkl) plane and Cu content.

Peak index	$2^{\theta_{avg}}$ (°)	ZnO	3%Cu_ZnO	3%Cu_ZnO	10%Cu_ZnO	Average ψ_{hkl}
		Shape factor (ψ_{hkl})				
(100)	31.773	0.6549	0.6895	0.6808	0.6891	0.6786(0.0163)
(002)	34.387	0.6551	0.6881	0.6807	0.6890	0.6782(0.0158)
(101)	36.251	0.6552	0.6871	0.6806	0.6890	0.6780(0.0156)
(102)	47.524	0.6562	0.6834	0.6803	0.6889	0.6772(0.0144)
(110)	56.619	0.6573	0.6823	0.6802	0.6889	0.6772(0.0137)
(103)	62.828	0.6582	0.6822	0.6801	0.6889	0.6774(0.0133)
(200)	66.408	0.6588	0.6824	0.6801	0.6890	0.6776(0.0131)
(112)	67.957	0.6589	0.6825	0.6801	0.6889	0.6776(0.0131)
(201)	69.115	0.6592	0.6826	0.6801	0.6890	0.6777(0.0129)
$\psi_{avg.}$		0.657(2)	0.684(3)	0.6804(3)	0.6889(6)	

Supplementary note 8:

Table. S7. Variation in Raman mode intensity (I) ratios given by: $E_1(LO)/E_2(high)$ and 2LO/LO with respect to crystallite size and Cu content

Sample ID	$E_1(LO)/E_2(high)$	2LO/LO	D (nm)
ZnO	0.2675 (0.0108)	2.40 (0.501)	53.4
3%Cu_ZnO	0.5589 (0.0409)	0.844 (0.087)	20.5
5%Cu_ZnO	0.4995 (0.0336)	0.748 (0.071)	21.5

Table. S8. Pearson IV profile parameters

Sample ID	Shape parameter (m)	Left width at half maxima (L_w)	Right width at half maxima (R_w)	Asymmetry L_w/R_w
ZnO	14.4	11.4542	8.5972	1.3323
3%Cu_ZnO	17.3	8.9086	7.2438	1.2298
5%Cu_ZnO	25.1	8.3465	6.6920	1.2472

References:

1. K. Vidhya, M. Saravanan, G. Bhoopathi, V. P. Devarajan, S. Subanya, Appl. Nanosci., 2015, 5, 235–243.
2. A. Sangeetha, S. Jaya Seeli, K. P. Bhuvana, M. Abdul Kader, S. K. Nayak, J. Solgel Sci. Technol., 2019, 91, 261–272.
3. S. Muthukumaran, R. Gopalakrishnan, Opt. Mater., 2012, 34, 1946–1953.
4. M. Darroudia, Z. Sabouri, R. K. Oskuee, A. K. Zak, H. Kargar, M. H. N. A. Hamid, Ceram. Int., 2014, 40, 4827–4831.
5. M. S. Corobea, A, M. Stoenescu, M. Miculescu, V. Raditoiu, R. C. Fierascu, I. Sirbu, Z. Vuluga, S. I. Voicu, Dig. J. Nanomater. Biostructures, 2014, 9, 1339 – 1347.
6. M. A. Zubair, M. T. Chowdhury, M. S. Bashar, M. A. Sami and M. F. Islam, *AIP Advances*, 2019, **9**, 045123